Optimal Energy Tradeoff among Communication, Computation and Caching with QoI-Guarantee

Faheem Zafari[1,*], Jian Li[2,*], Kin K. Leung[3], Don Towsley[4] and Ananthram Swami[5]

[1,3]Imperial College London, [2,4]University of Massachusetts Amherst, [5]U.S. Army Research Laboratory

[1,3]{faheem16, kin.leung}@imperial.ac.uk, [2,4]{jianli, towsley}@cs.umass.edu, [5]ananthram.swami.civ@mail.mil

*Co-primary authors

Abstract

Many applications must ingest and analyze data that are continuously generated over time from geographically distributed sources such as users, sensors and devices. This results in the need for efficient data analytics in geo-distributed systems. Energy efficiency is a fundamental requirement in these distributed systems, and its importance is reflected in much recent work on performance analysis of system energy consumption. However, most works have only focused on communication and computation costs, and do not account for caching costs. Given the increasing interest in cache networks, this is a serious deficiency. In this paper, we consider the energy consumption tradeoff between communication, computation, and caching (C3) for data analytics under a Quality of Information (QoI) guarantee in a geo-distributed system. To attain this goal, we formulate an optimization problem to capture the C3 costs, which turns out to be a non-convex Mixed Integer Non-Linear Programming (MINLP) Problem. We then propose a variant of spatial branch-and-bound algorithm (V-SBB), that can achieve ϵ-global[1] optimal solution to the original MINLP. We show numerically that V-SBB is more stable and robust than other candidate MINLP solvers under different network scenarios. More importantly, we observe that the energy efficiency under our C3 optimization framework improves by as much as 88% compared to any C2 optimization between communication and computation or caching.

Keywords

Energy Tradeoff, Data analytics, Data Caching, Quality of Information, Mixed Integer Non-Linear Programming, Spatial Branch-and-Bound

[1] ϵ-global optimality means that the obtained solution is within ϵ tolerance of the global optimal solution.

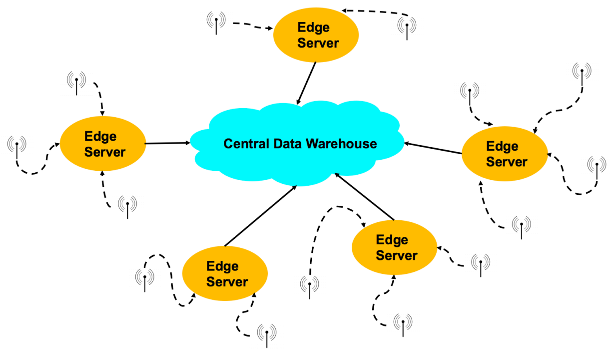

Fig. 1: The distributed model for a typical data analytics service consists of a single central and multiple edge servers in a hub-and-spoke architecture.

I. Introduction

Large quantities of data are generated continuously over time in the form of sensor reading, posts, emails etc. An efficient communication and processing system must provide efficient data analytics [1], [2] to extract useful and timely information for the user. Hence, there is a growing interest in designing distributed data analytics platforms [3].

In many data analytics systems, data is often generated and gathered from sources such as mobile devices, users and sensors at dispersed locations. As a result, the distributed infrastructure of a typical data analytics service (e.g., Google Analytics, Amazon Web Services etc) has a *hub-and-spoke* model (see Figure 1). Data are generated and sent to "edge" servers[2] near them. The edge servers are usually geographically distributed and process (e.g. compress) the incoming data and send the resultant data to other servers for further processing and storage.

While each server is able to process and store data, its resources are typically limited. In particular, the storage capacity and available power for data compression may be limited. It has been reported that the average annual power consumption for data analytics was 25 Giga-Watts in 2013 [4], [5], which is equivalent to operating 23 nuclear reactors. This not only increases the operational costs but also has an adverse environmental impact. Energy consumption is also a fundamental challenge for many wireless components that operate on limited battery power supply and are usually deployed in remote or inaccessible areas. Furthermore, about 5 zetta-bytes of data pass through the global network in 2017 [6]. This not only requires a huge network bandwidth, but may further increase the energy expenditure as communicating such a large amount of data in a distributed environment incurs tremendous transmission

[2] In this paper, we interchange the notion of (center and edge) server and node.

costs. These challenges necessitate the need for designs that can enhance the energy efficiency of distributed system with a QoI guarantee.

Typically there are two approaches to data analytics. On one hand, a *centralized approach* can be applied where all the collected data is sent to the centralized server and no processing is performed at the edge or intermediate nodes. However, such a centralized approach is often suboptimal and even infeasible, since it may cause large delay due to the limited communication bandwidth and does not make use of the available computation and storage resources at edges. On the other hand, a *decentralized approach* utilizes the edge resources to compute and store the data to reduce the network traffic. In this paper, we argue that data analytics must utilize both edges and center resources in a well-organized coordinated manner so as to achieve the minimal energy consumption by proper tradeoffs among data communication, computation and caching while satisfying stringent quality-of-information (QoI) requirements of the end users.

Data computation has been widely used in data analytics systems. It combines and compresses large quantities of generated data from data generators that must be processed in a specified time period. For example, Google Analytics can compute the total visits to one website from different regions and aggregate the visitors' information on an hourly basis. Data compression (computation) can lower transmission cost by removing the inherent redundancy in the data and reducing the total amount of data for further transmission at the expense of computational cost.

Furthermore, cache has become an important component of data analytics systems to store information locally. For instance, users in a geographical area want to receive the same information (e.g., live videos, commentary) generated by a number of data sources. In such cases, caching can be used as a mean to reduce the access latency (resulting in enhanced QoI) by storing the data generated in a finite period at some locations to serve the users. This can also help reduce the energy cost and bandwidth consumption as data are stored closer to the requesting nodes, eliminating the need for repeated transmissions from the source nodes that may be far away from the requesting users. For example, caches have been widely used in wireless sensor networks (WSNs) and its functionality in minimizing latency and reducing energy cost has been studied in [7]–[9]. However, data caching also consumes energy [10].

Due to the inter-dependence, there exists a tradeoff among data communication, computation and caching energy costs. In this paper, we formulate an optimization problem that characterizes the tradeoff among communication, computation, and caching energy cost with QoI guarantee, and then develop an efficient algorithm to solve the optimization problem. *Our algorithm decides how much data compression should be performed at each node and where data should be cached in the system.* Without loss of generality (W.l.o.g.), each node is assumed to have ability to compress and cache data up to some finite storage capacity.

A. Motivation

The setting of interest in this paper consists of a large number of (edge and center) servers, each equipped with finite storage capacity and data computation capability. Examples of such settings are WSNs, smart cities or Internet of Things (IoTs) where geographically distributed servers generate a large amount of data. In this paper, we focus on WSNs, particularly in the context of tactical environments [11] as an illustrative example. Wireless sensors are significant components in tactical environments which have limited bandwidth, energy resources but stringent requirements (e.g., low latency). In WSNs, sensors generate, process and transmit data to nearby edge servers, which can further process the data. As shown in Figure 1, we consider a tree-structured geo-distributed WSN. All sensors are battery operated and thus have limited power supply. W.l.o.g, data is generated only by the leaf nodes (sensors) and the goal of the network is to process the generated data while it is being forwarded toward the sink (root) node. The network also contains relay nodes that do not produce their own data, but can compress and cache data received from their corresponding children nodes. The sink node also receives and serves the requests for the data generated in this network. The relay nodes allow the leaf nodes to transmit over shorter range, hence reducing the energy consumption of the leaf nodes. Furthermore, the wireless channel conditions may also not be suitable for long range communications. The relay nodes transmit the data up the tree until it reaches the root node that satisfies any requests for the data of any particular leaf node. To continue, let us describe several key terms as follows.

Computation: Data aggregation [12], [13] is the process of gathering data from multiple generators (e.g., sensors), compressing them to eliminate redundant information and then providing the summarized information to end users. Since only part of the original data is transmitted, data aggregation can conserve a large amount of energy. A common assumption in previous work is that the amount of energy consumed by data compression is smaller than that needed to transmit the same amount of data. Therefore, data compression was considered a viable technique for reducing energy consumption. However, it has been shown [14] that computational energy cost can be significant and may cause a net-energy increase if data are compressed beyond a certain level (threshold). Hence, it is necessary to jointly consider both transmission and computation costs, and it is important to characterize the tradeoff between them [15].

Caching: Cache has been widely used in networks and distributed systems to improve performance by storing information locally, which jointly reduces access latency and bandwidth requirements, and hence improves user experience. The basic idea behind caching is to make information available at a location closer to the user. Again, most previous work focused on designing caching algorithms to enhance system performance without considering the energy cost of caching. However, caching itself can incur significant energy costs [16]. Therefore, capturing caching cost and characterizing the tradeoff between communication and caching energy cost are also critical for system design.

Quality of Information (QoI): The notion of QoI required by end users is affected by many factors. In particular, the degree of the data aggregation in a system is crucial for QoI. It has been shown that data aggregation can deteriorate QoI in some situations [17]. Thus an energy efficient design for appropriate data aggregation with a guaranteed QoI is desirable.

The objective of this work is to develop an efficient algorithm to minimize the total energy cost by incorporating data communication, computation and caching energy costs with a desired QoI constraint into our formulation, so that the optimal data compression rate at each node and the optimal data caching location in the network can be determined. Such an algorithm should be lightweight and achieve the optimal solution efficiently.

B. Organization and Main Results

In Section II, we describe our system model in which nodes are logically arranged as a tree. Each node receives and compresses data from its children node(s). The compressed data are transmitted and further compressed by upstream nodes towards the sink node. Each node can also cache the compressed data locally. In Section III, we formulate the problem of energy-efficient data compression, communication and caching with QoI constraint as a non-convex mixed integer non-linear programming (MINLP) problem, which is hard to solve in general. We then show that there exists an equivalent problem obtained through symbolic reformation [18] in Section IV, and propose a variant of the Spatial Branch-and-Bound (V-SBB) algorithm to solve it. We show that our proposed algorithm can achieve ϵ-global optimality of the original MINLP efficiently. Since we have a discrete space and a non-convex problem, showing that there exists an ϵ-optimal solution and developing an efficient algorithm to achieve it are quite intricate. This is another contribution in this paper.

In Section V, we evaluate the performance of our optimization framework and the proposed V-SBB algorithm through extensive numerical studies. In particular, we make a thorough comparison with other MINLP solvers Bonmin [19], NOMAD [20], and Matlab's genetic algorithm (GA) under different network scenarios. The results show that our algorithm can achieve the ϵ-global optimality, and is either comparable to or outperforms Bonmin. Furthermore, our algorithm is more robust and stable in the context of varying network situations. In other words, Bonmin in certain cases is not able to provide a solution, even though the original problem is feasible. Furthermore, our algorithm easily outperforms NOMAD and Matlab's GA [21] in most of our testing scenarios. More importantly, we observe that with the joint optimization

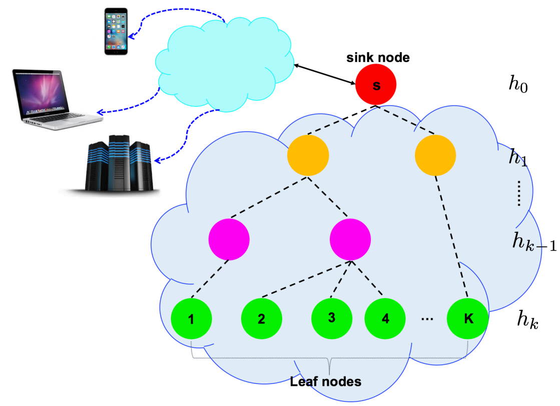

Fig. 2: Tree-Structured Network Model.

of data communication, computation and caching (C3), energy efficiency can be improved by as much as 88% compared to only optimizing communication and computation, or communication and caching (C2). This further strengthens the contributions of our optimization framework of C3. In Section VI, we review previous work, and conclude in Section VII.

II. Analytical Model

We represent the network as a directed graph $G = (V, E)$. As shown in Section I, a hub-and-spoke model shown in Figure 1 usually exists in data analytics systems including WSNs. W.l.o.g., we consider a tree, with $N = |V|$ nodes, as shown in Figure 2. Node $v \in V$ is capable of storing S_v amount of data. Let $\mathcal{K} \subseteq V$ with $K = |\mathcal{K}|$ be the set of leaf nodes, with $\mathcal{K} = \{1, 2, \cdots, K\}$. Time is partitioned in periods of equal length $T > 0$ and data generated in each period are independent, i.e., the transmitted and cached data in one time period may be totally replaced with new data for the next time period[3]. W.l.o.g., we consider one particular period in the remainder of the paper. As is the case in a typical geo-distributed analytics system, we assume that only leaf nodes $k \in \mathcal{K}$ can generate data, and all other nodes in the tree receive and compress data from their children nodes, and either cache or transmit the compressed data to their parent nodes during time T. Relaxation of the preceding assumptions is discussed in Section III-B.

Let y_k be the amount of data generated by leaf node $k \in \mathcal{K}$. The data generated at the leaf nodes are transmitted up the tree to the sink node s, which serves the requests for the data generated in the network. Let $h(k)$ be the depth of node k in the tree. W.l.o.g., we assume that the sink node is located at level $h(s) = 0$. We represent the unique path from node k to the sink node by $\mathcal{H}^k$ of length $h(k)$ the

[3]In some literature, this is called *windowed grouped data aggregation* where data generated in a finite time period must be compressed.

TABLE I: Summary of notations

Notation	**Description**
y_k	number of data (bits) generated at node k
y_v	number of data (bits) present at node v where $y_v = \prod_{j=h(k)}^{h(v)} \delta_{k,j} y_k$
$\delta_{k,v}$	reduction rate at node v, is the ratio of amount of output data to input data
γ	the QoI threshold
ε_{vR}	per-bit reception cost of node v
ε_{vT}	per-bit transmission cost of node v
ε_{vC}	per-bit compression cost of node v
$b_{k,v}$	1 if node v caches the data from leaf node k; otherwise 0
S_v	storage capacity of node v
w_{ca}	caching power efficiency
R_k	request rate for data from node k
N	total number of nodes in the network
C_v	set of leaf nodes that are descendants of node v
T	time length that data are cached
ϕ^u	upper bound of the objective function
$\mathcal{L}$	list of regions
$\mathcal{R}$	any sub-region in $\mathcal{L}$
$\phi^{\mathcal{R},u}$	upper bound on the objective function in subregion $\mathcal{R}$
$\phi^{\mathcal{R},l}$	lower bound on the objective function in subregion $\mathcal{R}$
ϵ	difference between the upper and lower bound

sequence $\{h_0^k, h_1^k, \cdots, h_{h(k)}^k\}$ of nodes $h_j^k \in V$ such that $(h_j^k, h_{j+1}^k) \in E$, where $h_0^k \triangleq s$ (i.e., the sink node) and $h_{h(k)}^k \triangleq k$ (i.e., the node itself).

We denote the per-bit reception, transmission and compression cost of node $v \in V$ as $\varepsilon_{vR}, \varepsilon_{vT}$, and ε_{vC}, respectively. Each node h_i^k along the path $\mathcal{H}^k$ can compress the data generated by leaf node k with a *data reduction rate* $\delta_{k,i}$ (ratio of the outgoing data from a node to the incoming data), where $0 < \delta_{k,i} \leq 1$, $\forall i, k$. The reduction rate characterizes the degree to which a node can compress the received data, which plays an important role for determining the QoI.

The higher the value of $\delta_{k,i}$, the lower the compression will be, and vice versa. The higher the degree of data compression, the larger will be the amount of energy consumed by compression. Similarly, caching the data closer to the sink node may reduce the transmission cost for serving the request, however, each node only has finite storage capacity. We study the tradeoff among the energy consumed at each node for transmitting, compressing and caching the data.

Denote the total energy consumption at node v as E_v, which consists of the reception cost E_{vR}, transmission cost E_{vT}, computation cost E_{vC} and storage (caching) cost E_{vS}; it takes the form

$$E_v = E_{vR} + E_{vT} + E_{vC} + E_{vS}, \tag{1}$$

where

$$E_{vR} = y_v \varepsilon_{vR}, \qquad E_{vT} = y_v \varepsilon_{vT} \delta_v,$$
$$E_{vC} = y_v \varepsilon_{vC} l_v(\delta_v), \qquad E_{vS} = w_{ca} y_v T. \tag{2}$$

Here, $l_v(\delta_v)$ captures the computation energy. As computation energy increases with the degree of compression, we assume that $l_v(\delta_v)$ is a continuous, decreasing and differentiable function of the reduction rate. One candidate function is $l_v(\delta_v) = 1/\delta_v - 1$ [15], [22]. Moreover, we consider an energy-proportional model [16] for caching, i.e., $E_{vS} = w_{ca} y_v T$ if the received data y_v is cached for a duration of T where w_{ca} represents the power efficiency of caching, which strongly depends on the storage hardware technology. W.l.o.g., w_{ca} is assumed to be identical for all the nodes. For simplicity, denote

$$f(\delta_v) = \varepsilon_{vR} + \varepsilon_{vT}\delta_v + \varepsilon_{vC} l_v(\delta_v), \tag{3}$$

as the sum of per-bit reception, transmission and compression cost at node v per unit time.

During time period T, we assume that there are R_k requests at the sink node s for data y_k generated by leaf node k[4]. We set the boolean variable $b_{k,i}$ to 1 if the data from node k is stored along the path $\mathcal{H}^k$ at node h_i^k, otherwise it equals 0. For ease of notation, we denote $b_{k,h(k)}$ by b_k, $f_{k,h(k)} \triangleq f_k$ and $\delta_{k,h(k)} \triangleq \delta_k$. Let C_v denote the set of leaf nodes $k \in \mathcal{K}$ that are descendants of node v.

We also assume that the energy cost for searching for data at different nodes in the network is negligible [15], [23]. For ease of exposition, the parameters used throughout this paper are summarized in Table I.

III. Energy Optimization

In this section, we first define the cost function in our model and then formulate the optimization problem. Data produced by every leaf node is received, transmitted, and possibly compressed by all nodes in the path from the leaf node to the root node, consuming energy

$$E_k^{\mathrm{C}} = \sum_{i=0}^{h(k)} y_k f(\delta_{k,i}) \prod_{m=i+1}^{h(k)} \delta_{k,m}, \tag{4}$$

where $\prod_{m=i}^{j} \delta_{k,m} := 1$ if $i \geq j$. Equation (4) captures one-time[5] energy cost of receiving, compressing and transmitting data y_k from leaf node (level $h(k)$) to the sink node (level 0). The amount of data

[4] As motivated in Section I, a large number of agents may desire the same information, hence there are multiple requests for the same data.

[5] During every time period T, data is always pushed towards the sink upon the first request.

received by any node at level i from leaf node k is $y_k \prod_{m=i+1}^{h(k)} \delta_{k,m}$ due to the compression from level $h(k)$ to $i+1$. The term $f(\delta_{k,i})$ captures the reception, transmission and compression energy cost for node at level i along the path from leaf node k to the sink node.

Let E_k^{R} be the total energy consumed in responding to the subsequent (R_k-1) requests. We have

$$E_k^{\text{R}} = \sum_{i=0}^{h(k)} y_k(R_k-1)\left\{ f(\delta_{k,i}) \prod_{m=i+1}^{h(k)} \delta_{k,m}\left(1-\sum_{j=0}^{i} b_{k,j}\right) + \left(\prod_{m=i}^{h(k)} \delta_{k,m}\right) b_{k,i}\left(\frac{w_{ca}T}{R_k-1}+\varepsilon_{kT}\right)\right\}. \quad (5)$$

Note that the remaining (R_k-1) requests are either served by the leaf node or a cached copy of data y_k at level i for $i=1,\cdots,h(k)$. W.l.o.g., we consider node $v_{k,i}$ at level i. If data y_k is not cached from $v_{k,i}$ up to the sink node (level 0), i.e., $b_{k,j}=0$ for $j=0,\cdots,i$, the cost is incurred due to receiving, transmitting and compressing the data (R_k-1) times, which is captured by the first term in Equation (5), the second term is 0. Otherwise, the (R_k-1) requests are served by the cached copy at $v_{k,i}$, the corresponding caching and transmission cost serving from $v_{k,i}$ are captured by the second term in Equation (5), and the corresponding reception, transmission and compression cost from $v_{k,i-1}$ upto to sink node is captured by the first term. Note that the first time cost of reception, transmission and compression the data from leaf node to $v_{k,i}$ is already captured by Equation (4).

We present a simple but illustrative example to explain the above equations.

Example 1. *We consider a network with one leaf node and one sink node, i.e.,* $k=1$ *and* $h(k)=1$*. Then the cost in Equation (4) becomes* $E_1^C = y_1 f(\delta_{1,0})\delta_{1,1} + y_1 f(\delta_{1,1})$*, where the first and second terms capture the reception, transmission and compression cost for data* y_1 *at sink node and the leaf node, respectively.*

The cost in Equation (5) is $E_1^R =$

$$\underbrace{y_1(R_1-1)\left[f(\delta_{1,0})\delta_{1,1}(1-b_{1,0}) + \delta_{1,0}\delta_{1,1}b_{1,0}\left(\frac{w_{ca}T}{R_1-1}+\varepsilon_{1T}\right)\right]}_{\textit{Term } 1}$$
$$+\underbrace{y_1(R_1-1)\left[f(\delta_{1,1})(1-b_{1,0}-b_{1,1}) + \delta_{1,1}b_{1,1}\left(\frac{w_{ca}T}{R_1-1}+\varepsilon_{1T}\right)\right]}_{\textit{Term } 2},$$

where Term 1 *and Term* 2 *capture the costs at sink node and leaf node, respectively. To be more specific, there are three cases: (i) data* y_1 *is cached at sink node* 0*, i.e.,* $b_{1,0}=1$ *and* $b_{1,1}=0$ *(since we only cache one copy); (ii) data* y_1 *is cached at leaf node* 1*, i.e.,* $b_{1,0}=0$ *and* $b_{1,1}=1$*; and (iii) data* y_1 *is not cached, i.e.,* $b_{1,0}=b_{1,1}=0$*. We consider these three cases in the following.*

Case (i), i.e., $b_{1,0}=1$ *and* $b_{1,1}=0$*, Term* 2 *becomes* 0 *and Term* 1 *reduces to* $y_1(R_1-1)\delta_{1,0}\delta_{1,1}b_{1,0}(\frac{w_{ca}T}{R_1-1}$ $+\varepsilon_{1T})$ *since all the* (R_1-1) *requests are served from sink node. This indicates that the total energy* *cost is due to caching the data for time period T and transmitting it $(R_k - 1)$ times from the sink node to users that request it.*

Case (ii), i.e., $b_{1,0} = 0$ and $b_{1,1} = 1$, Term 1 becomes $y_1(R_1 - 1)f(\delta_{1,0})\delta_{1,1}$, which captures the reception, transmission and compression costs at sink node 0 for serving the $(R_1 - 1)$ requests. Term 2 becomes $y_1(R_1-1)\delta_{1,1}b_{1,1}\left(\frac{w_{ca}T}{R_1-1} + \varepsilon_{1T}\right)$, which captures the cost of caching data at the leaf node and transmitting the data $(R_k - 1)$ times from the cached copy to the sink node . The sum of them is the total cost to serve $(R_1 - 1)$ requests.

Case (iii), i.e., $b_{1,0} = b_{1,1} = 0$, $E_1^R = y_1(R_1 - 1)f(\delta_{1,0})\delta_{1,1} + y_1(R_1 - 1)f(\delta_{1,1})$, which captures the reception, transmission and compression costs at sink node 0 and leaf node 1 for serving the $(R_1 - 1)$ requests since there is no cached copy in the network.

The total energy consumed in the network is E^{total},

$$E^{\text{total}}(\boldsymbol{\delta}, \boldsymbol{b}) \triangleq \sum_{k\in\mathcal{K}} \left(E_k^{\text{C}} + E_k^{\text{R}} \right), \tag{6}$$

where $\boldsymbol{\delta} = \{\delta_{k,i}, \forall k \in \mathcal{K}, i = 0, \cdots, h(k)\}$ and $\boldsymbol{b} = \{b_{k,i}, \forall k \in \mathcal{K}, i = 0, \cdots, h(k)\}$. Our objective is to minimize the total energy consumption of the network with a QoI constraint for end users by choosing the compression ratio vector $\boldsymbol{\delta}$ and caching decision vector $\boldsymbol{b}$ in the network G. Therefore, the optimization problem is,

$$\begin{aligned}
\min_{\boldsymbol{\delta},\boldsymbol{b}} \quad & E^{\text{total}}(\boldsymbol{\delta}, \boldsymbol{b}) \\
\text{s.t.} \quad & \sum_{k\in\mathcal{K}} y_k \prod_{i=0}^{h(k)} \delta_{k,i} \geq \gamma, \\
& b_{k,i} \in \{0,1\}, \forall k \in \mathcal{K}, i = 0, \cdots, h(k), \\
& \sum_{k\in C_v} b_{k,h(v)} y_k \prod_{j=h(k)}^{h(v)} \delta_{k,j} \leq S_v, \forall\, v \in V, \\
& \sum_{i=0}^{h(k)} b_{k,i} \leq 1, \forall k \in \mathcal{K},
\end{aligned} \tag{7}$$

where $h(v)$ is the depth of node v in the tree.

The first constraint is the QoI constraint, i.e., the total data available at the sink node [15]. The second constraint indicates that our decision (caching) variable $b_{k,i}$ is binary. The third constraint is on total amount of data that can be cached at each node. The fourth constraint is that at most one copy of the generated data should be cached on the path between the leaf node and the sink node.

The optimization problem in (7) is a non-convex MINLP problem with M continuous variables, the $\delta_{k,i}$'s and M binary variables, the $b_{k,i}$'s where, $M = \sum_{k\in\mathcal{K}} h(k)$.

A. Properties

Theorem 1. *The optimization problem defined in* (7) *is NP-hard.*

Proof. The optimization problem (7) can be reduced to a general non-convex MINLP problem as shown in Appendix A. Since non-convex MINLP is NP-hard [24], the optimization problem described in (7) is NP-hard. □

Remark 1. *The objective function E^{total} defined in* (7) *is monotonically increasing in the number of requests R_k for all $k \in \mathcal{K}$ provided that $\boldsymbol{\delta}$ and $\boldsymbol{b}$ are fixed.*

Notice that (4) is independent of R_k and (5) is linear in R_k, and its multipliers are positive. Hence, for any fixed $\boldsymbol{b}$ and $\boldsymbol{\delta}$, (6) increases monotonically with R_k.

Remark 2. *Given a fixed network scenario, if we increase the number of requests R_k for the data generated by leaf node k, then these data will be cached closer to the sink node or at the sink node, if there exists enough cache capacity, to reduce the overall energy consumption.*

For fixed $\boldsymbol{\delta}$, observe from (5) that energy consumption decreases if the cache is moved closer to the root as the nodes deep in the tree do not need to retransmit.

B. Relaxation of Assumptions

In our model, we make several assumptions for the sake of simplicity. In the following, we discuss the relaxation of these assumptions.

While we assume that the network is structured as a tree, this assumption can be easily relaxed as long as there exists a simple fixed path from each leaf node to the sink node. The tree structure represents a simple topology that captures the key parameters in the optimization formulation without the complexity introduced by a general network topology. Furthermore, for simplicity, we assume that all parameters across the nodes are identical, which is not necessary as seen from the cost function. We also assume that only leaf nodes generate data. However, our model can be extended to allow intermediate nodes to generate data at the cost of added complexity.

IV. Variant of Spatial Branch-and-Bound Algorithm

In this section, we present a variant of the Spatial Brand-and-Bound algorithm (V-SBB). Instead of solving the MINLP problem (7) directly, we use V-SBB to solve a *standard form* of the original MINLP. We first introduce the *Symbolic Reformulation* [18] method that reformulates the MINLP (7) into a standard form needed by V-SBB.

Definition 1. *A MINLP problem is said to be in a* standard form *if it can be written as*

$$
\begin{aligned}
\min_{\boldsymbol{w}} \quad & \boldsymbol{w}_{obj} \\
\textit{s.t.} \quad & \mathbf{A}\mathbf{w} = \mathbf{b}, \\
& \mathbf{w}^{l} \leq \mathbf{w} \leq \mathbf{w}^{U}, \\
& \mathbf{w}_k \equiv \mathbf{w}_i \mathbf{w}_j, \quad \forall (i,j,k) \in \mathcal{T}_{bt}, \\
& \mathbf{w}_k \equiv \mathbf{w}_i / \mathbf{w}_j, \quad \forall (i,j,k) \in \mathcal{T}_{lft},
\end{aligned} \tag{8}
$$

where the vector of variables $\mathbf{w}$ consists of continuous and discrete variables in the original MINLP. The sets τ_{bt} and τ_{lft} contain all relationships that arise in the reformulation. $\boldsymbol{A}$ and $\boldsymbol{b}$ are a matrix and a vector of real coefficients, respectively. The index obj denotes the position of a single variable corresponding to the objective function value within the vector $\boldsymbol{w}$.

Theorem 2. *The non-convex MINLP problem (7) can be transformed into a standard form.*

Due to space constraints, we relegate detailed reformulations and standard form of (7) to Appendix B. Here, we give an example to illustrate the above reformulation process.

Example 2. Consider the same network in Example 1, the non-convex MINLP problem becomes

$$
\begin{aligned}
\min_{\boldsymbol{\delta}, \boldsymbol{b}} \quad & E^{\text{total}}(\boldsymbol{\delta}, \boldsymbol{b}) = E_1^C + E_1^R \\
\text{s.t.} \quad & y_1 \delta_{1,0} \delta_{1,1} \geq \gamma, \\
& b_{1,0}, b_{1,1} \in \{0,1\}, \\
& b_{1,0} y_1 \delta_{1,0} \delta_{1,1} \leq S_0, \\
& b_{1,1} y_1 \delta_{1,1} \leq S_1, \\
& b_{1,0} + b_{1,1} \leq 1.
\end{aligned} \tag{9}
$$

$\delta_{1,0}\delta_{1,1}$ is a bilinear term. Based on symbolic reformulation rules, a new bilinear auxiliary variable $w_{1,0}^{\text{bt}}$ needs to be added. The first constraint in (9) is then transformed into $y_1 w_{1,0}^{\text{bt}} \geq \gamma$, which is linear in auxiliary variable $w_{1,0}^{\text{bt}}$. Similarly, we add $w_{1,0}^{\text{lft}}$ for linear-fractional term $\delta_{1,1}/\delta_{1,0}$ that appears in $f(\cdot)$. $b_{1,0}\delta_{1,0}\delta_{1,1}$ in the third constraint of (9) is a tri-linear term. Since $\delta_{1,0}\delta_{1,1}$ is replaced by $w_{1,0}^{\text{bt}}$, we obtain a bilinear term $b_{1,0}w_{1,0}^{\text{bt}}$. Again, based on symbolic reformulation rules, $b_{1,0}w_{1,0}^{\text{bt}}$ is replaced by a new auxiliary variable $\overline{w}_{1,0}^{\text{bt}}$. Similarly we add new auxiliary variables $\tilde{w}_{1,1}^{\text{b}}, \tilde{w}_{1,0}^{\text{bt}},, \tilde{w}_{1,0}^{\text{lft}}$ and $\tilde{w}_{1,1}^{\text{lft}}$. The objective function in (9) can be then expressed as a function of these new auxiliary variables. Therefore, the standard form of (9) is

$$
\begin{aligned}
\min_{\boldsymbol{\delta},\boldsymbol{b}} \quad & w_{\text{obj}} \\
\text{s.t.} \quad & y_1 w_{1,0}^{\text{bt}} \geq \gamma, \\
& b_{1,0}, b_{1,1} \in \{0,1\}, \\
& y_1 \overline{w}_{1,0}^{\text{bt}} \leq S_0, \\
& y_1 \tilde{w}_{1,1}^{\text{bt}} \leq S_1, \\
& b_{1,0} + b_{1,1} \leq 1, \\
& w_{1,0}^{\text{bt}} = \delta_{1,1} \times \delta_{1,0}, \\
& w_{1,0}^{\text{lft}} = \delta_{1,1}/\delta_{1,0}, \\
& \overline{w}_{1,0}^{\text{bt}} = b_{1,0} \times w_{1,0}^{b}, \\
& \tilde{w}_{1,1}^{\text{bt}} = b_{1,1} \times \delta_{1,1}, \\
& \tilde{w}_{1,0}^{\text{bt}} = \delta_{1,1} \times b_{1,0}, \\
& \tilde{w}_{1,0}^{\text{lft}} = b_{1,0}/\delta_{1,1}, \\
& \overline{w}_{1,0}^{\text{lft}} = b_{1,0} w_{1,0}^{\text{lft}}, \\
& \tilde{w}_{1,1}^{\text{lft}} = b_{1,1}/\delta_{1,1}, \\
& w_{\text{obj}} = y_1 \varepsilon_{1R} \delta_{1,1} + \varepsilon_{1T} y_1 w_{1,0}^{\text{bt}} + y_1 \varepsilon_{1C} w_{1,0}^{\text{lft}} - y_1 \varepsilon_{1C} \delta_{1,1} + y_1 \varepsilon_{1R} \varepsilon_{1T} y_1 \delta_{1,1} + y_1 \varepsilon_{1C}/\delta_{1,1} - y_1 \varepsilon_{1C} + \\
& y_1 (R_1 - 1) \Big(\varepsilon_{1R} \delta_{1,1} + \varepsilon_{1T} w_{1,0}^{\text{bt}} - \varepsilon_{1C} \delta_{1,1} + \varepsilon_{1C} w_{1,0}^{\text{lft}} - \varepsilon_{1R} \tilde{w}_{1,0}^{\text{bt}} - \varepsilon_{1T} \overline{w}_{10}^{\text{bt}} + \varepsilon_{1C} \tilde{w}_{1,0}^{\text{bt}} - \varepsilon_{1C} \overline{w}_{1,0}^{\text{lft}} \Big) + \\
& y_1 (R_1 - 1) \varepsilon_{1T} + y_1 w_{ca} T \overline{w}_{1,0}^{\text{bt}} + y_1 (R_1 - 1) \Big(\varepsilon_{1R} - \varepsilon_{1C} + \varepsilon_{1T} \delta_{1,1} + \varepsilon_{1C}/\delta_{1,1} - \varepsilon_{1R} b_{1,0} - \varepsilon_{1C} b_{1,0} - \\
& \varepsilon_{1T} \tilde{w}_{1,0}^{\text{bt}} - \varepsilon_{1C} \tilde{w}_{1,0}^{\text{lft}} - \varepsilon_{1R} b_{1,1} + \varepsilon_{1C} b_{1,1} - \varepsilon_{1T} \tilde{w}_{1,1}^{\text{bt}} - \varepsilon_{1C} \tilde{w}_{1,1}^{\text{lft}} \Big).
\end{aligned} \tag{10}
$$

Through this reformulation, the non-convex and non-linear terms in the original problem are transformed into bilinear and linear fractional terms, which can be easily used to compute the lower bound of each region in V-SBB, which are discussed in details later. This is the reason V-SBB requires reformulating the original problem into a standard form.

Theorem 3. *Reformulated problem and the original MINLP are equivalent.*

Proof is available in Section 2 (page 460) [18].

Due to the reformulation, the number of variables in the reformulated problem is larger than in the original MINLP. In the following, we show that the number of auxiliary variables that arise from symbolic reformulation is bounded.

Remark 3. *The number of auxiliary variables in the symbolic reformulation is $O(n^2)$, where $n = 2M$ is the number of variables in the original formulation.*

From [25], a way to transform a general form optimization problem into a standard form (8) is through basic arithmetic operations on original variables. To be more specific, any algebraic expression results from the basic operators including the five basic binary operators, i.e., addition, subtraction, multiplication, division and exponentiation, and the unary operators, i.e., logarithms etc. Therefore, in order to construct a standard problem consisting of simple terms corresponding to these binary or unary operations, new variables need to be added corresponding to these operations. From the symbolic reformulation process [25]–[27], any added variable results from the basic operations between two (including possibly the same) original variables or added variables. Hence, based on the basic operations, there are at most n^2 combinations of these variables, given that there are n variables in the original problem (7). Therefore, the number of added variables in the symbolic reformulation is bounded as $O(n^2)$. In the remainder of this section, we present the V-SBB to solve the equivalent problem.

Algorithm 1 Variant of Spatial Branch-and-Bound (V-SBB)

Step 1: Initialize $\phi^u := \infty$ and $\mathcal{L}$ to a single domain

Step 2: Choose a subregion $\mathcal{R} \in \mathcal{L}$ using *least lower bound rule*

if $\mathcal{L}$ = $\emptyset$ **then** Go to Step 6

if for chosen region $\mathcal{R}$, $\phi^{\mathcal{R},l}$ is infeasible or $\phi^{\mathcal{R},l} \geq \phi^u - \epsilon$ **then** Go to Step 5

Step 3: Obtain the upper bound $\phi^{\mathcal{R},u}$

if upper bound cannot be obtained or if $\phi^{\mathcal{R},u} > \phi^u$ **then** Go to Step 4

else $\phi^u :=\phi^{\mathcal{R},u}$ and, from the list $\mathcal{L}$, delete all subregions $\mathcal{S} \in \mathcal{L}$ such that $\phi^{\mathcal{S},l} \geq \phi^u - \epsilon$

if $\phi^{\mathcal{R},u} - \phi^{\mathcal{R},l} \leq \epsilon$ **then** Go to Step 5

Step 4: Partition $\mathcal{R}$ into new subregions $\mathcal{R}_{\text{right}}$ and $\mathcal{R}_{\text{left}}$

Step 5: Delete $\mathcal{R}$ from $\mathcal{L}$ and go to Step 2

Step 6: Terminate Search

if $\phi^u = \infty$ **then** Problem is infeasible

else ϕ^u is ϵ-global optimal

A. Our Variant of Spatial Branch-and-Bound

The proposed spatial branch-and-bound method is a variant of the method proposed in [25] and is primarily tuned for solving our optimization problem (16) that is also the solution of (7). Our algorithm is different from [25] because

- We do not use any bounds tightening steps as it does not always guarantee faster convergence [28] and in case of our problem slowed down the process.
- By eliminating the bounds tightening step, we do not need to calculate the lower bound $\phi^{\mathcal{R},l}$ again separately and utilize the lower bound obtained in Step 2 for the chosen region $\mathcal{R}$, hence reducing the computational complexity of the algorithm.

Algorithm 1 provides an overview of the steps involved in spatial branch-and-bound algorithm. We describe some of the steps in Algorithm 1 in detail below.

Step 2*:* There are a number of approaches that can be used to choose a subregion $\mathcal{R}$ from $\mathcal{L}$ [24]. Here we use the *least lower bound rule*, i.e., we choose a subregion $\mathcal{R} \in \mathcal{L}$ that has the lowest lower bound among all the subregions, since it is a widely used and well researched method. The lower bound can be obtained by solving a convex relaxation of the problem in (16). As our optimization problem in (7) and (16) contains only bilinear and linear fractional terms, we use McCormick linear over-estimators and under-estimators [29] (see Appendix C) to obtain a convex relaxation of all such terms. The resulting problem is then a Mixed Integer Linear Programming (MILP) problem that we solve using the *SCIP* solver [30]. The SCIP solver is a faster and well known solver for MILP problems. The subregion with lowest lower bound is then used as the region to explore for an optimum. The chosen regions' lower bound is used as $\phi^{\mathcal{R},l}$. If the convex relaxation is infeasible or if the obtained lower bound is higher than the existing upper bound ϕ^u of the problem, we *fathom* or delete the current region by moving to step 5.

Step 3*:* In step 3, we calculate the upper bound $\phi^{\mathcal{R},u}$ for the subregion $\mathcal{R}$ chosen in Step 2. This can be done in a number of ways (see [25]), here we use local MINLP solver such as *Bonmin* [19] to obtain a local minimum for the subregion as it performed better in terms of time than using local non-linear programming optimization with fixed discrete values or added discreteness constraints in our simulation settings. If the upper bound for the region $\phi^{\mathcal{R},u}$ cannot be obtained or if it is greater than ϕ^u then we move to Step 4 to further divide the region and search further for a better solution. Otherwise we set it as the current best solution ϕ^u and delete all the subregions whose lower bound is greater than the obtained upper bound since all such regions cannot contain the ϵ-global optimal solution. If the difference between the upper and lower bound for the region is within the ε-tolerance, the current subregion need not to be searched further, then we delete the current subregion by going to step 5, otherwise we move to step 4 for further searching in the space.

Step 4*:* Step 4 also known as the branching/partitioning step helps in partitioning/dividing a region to further refine the search for solution. In branching step, we select a variable for branching/partitioning as well as the value of the variable at which the region is to be divided. There are a number of different rules and techniques that can be used for branching (see [24] for detailed discussion). Here we use the variable selection and value selection rule specified in [26], since it has been found efficient for our problem [26].

We branch on the variable that causes the maximum reduction in the feasibility gap between the solution of convex relaxation (solution of Step 2) and the exact problem. To do so, the approximation error for the bilinear and linear fractional terms in (16) is calculated using (11a) and (11b) respectively where $\mathcal{S}_2$ means the value of the variable obtained in Step 2. The variable with the maximum approximation error of all is chosen as the branching variable as that tightens the gap between the relaxation and the exact problem [26]. This results in two candidate variables for branching i.e. w_i and w_j. If one of the variables is discrete (binary in our case) and the other is continuous then choose the discrete variable since it will result only in finite number of branches. However, if both variables are of the same type (either binary or continuous), then the branching variable is chosen using (12) i.e. we choose the variable w_b that has its value $w_b^{\mathcal{R}}$ closer to its range's midpoint. However, we first need to obtain the branching value for the candidate variables w_{bc}^{∇} (the value at which to branch). w_{bc}^{∇} should be between the upper and lower bounds of the variable in the region i.e. $w_{bc}^{\nabla,l} < w_{bc}^{\nabla} < w_{bc}^{\nabla,u}$. The rules for the choice of the branch point have been set in [26], however we restate them here for sake of completeness.

- Set w_{bc}^{∇} to the value obtained in Step 2, i.e., $w_{bc}^{\nabla} := w_{bc}^{\mathcal{S}_2}$.
- If any feasible upper bound $\phi^u = \phi(w_{bc}^*)$ has been obtained and $w_{bc}^{\nabla,l} < w_{bc}^* < w_{bc}^{\nabla,u}$, then $w_{bc}^{\nabla} := w_{bc}^*$ and stop the search for the value.
- If step 4 provided an upper bound $\phi^{\mathcal{R},u}$ for the subregion $\mathcal{R}$, then $w_{bc}^{\nabla} := w_{bc}^{\mathcal{R}}$.

After obtaining the branch point value, we have all the parameters required for (12) and can then choose the variable for branching.

$$E_{\text{bt}}^{ijk} = |w_k^{\mathcal{S}_2} - w_i^{\mathcal{S}_2} w_j^{\mathcal{S}_2}| \ \forall (i,j,k) \ \in \ \mathcal{T}_{\text{bt}} \tag{11a}$$

$$E_{\text{lft}}^{ijk} = \left| w_k^{\mathcal{S}_2} - \frac{w_i^{\mathcal{S}_2}}{w_j^{\mathcal{S}_2}} \right| \ \forall (i,j,k) \ \in \ \mathcal{T}_{\text{lft}} \tag{11b}$$

$$w_b = \arg\ \min \left\{ \left| 0.5 - \left(\frac{w_i^{\nabla} - w_i^{\mathcal{R},l}}{w_i^{\mathcal{R},u} - w_i^{\mathcal{R},l}} \right) \right|, \left| 0.5 - \left(\frac{w_j^{\nabla} - w_j^{\mathcal{R},l}}{w_j^{\mathcal{R},u} - w_j^{\mathcal{R},l}} \right) \right| \right\} \tag{12}$$

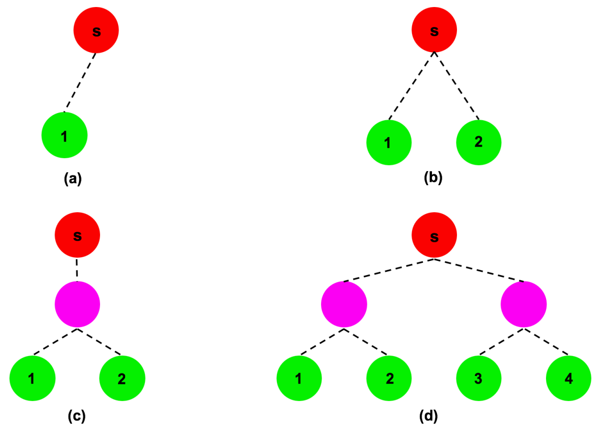

Fig. 3: Candidate network topologies used in the experiments: (a) one sink node and one leaf node; (b) one sink node and two leaf nodes; (c) one sink node, one intermediate node and two leaf nodes; and (d) one sink node, two intermediate nodes and four leaf nodes.

We partition the subregion $\mathcal{R}$ into $\mathcal{R}_{\text{right}}$ and $\mathcal{R}_{\text{left}}$ and add $\mathcal{R}_{\text{right}}$, $\mathcal{R}_{\text{left}}$ into our region list $\mathcal{L}$. Then we move to *Step* 5 and delete the subregion $\mathcal{R}$ from the list $\mathcal{L}$.

B. Convergence of Spatial Branch-and-Bound

The spatial branch-and-bound method guarantees convergence to ϵ-global optimality, which has been proven in [28]. However, for sake of completeness, we restate the proof in the Appendix D.

V. Evaluation

We evaluate the performance of our V-SBB algorithm as well as the energy efficiency of our communication, compression and caching (C3) joint optimization framework through a series of experiments on several network topologies as shown in Figure 3. Our key objective is to gain preliminary insights into our algorithm when compared with a few other well-known techniques. The highlights of the evaluation results are:

- Our V-SBB algorithm can obtain an ϵ-global optimal solution in most situations within a reasonable time. Also it is robust and stable to various parameters in different network scenarios.
- When Bonmin [19] can achieve a solution, it is faster. However, the solution obtained through Bonmin is not always comparable to that of V-SBB. We observe that when higher compression is done (i.e., smaller value of γ), V-SBB always outperforms Bonmin. More importantly, we find that Bonmin has poor performance in stability and robustness, i.e., it cannot even produce feasible solutions in

some cases although they exist. NOMAD [20] and GA [21] often produce objective-function values much larger than V-SBB.

- Our C3 joint optimization framework improves energy efficiency by as much as 88% compared to the C2 optimization over communication and computation, or communication and caching.

TABLE II: Characteristics of the solvers used in this paper

Solver	Characteristics
Bonmin [19]	A deterministic approach based on Branch-and-Cut method that solves relaxation problem with Interior Point Optimization tool (IPOPT), as well as mixed integer problem with Coin or Branch and Cut (CBC).
NOMAD [20]	A stochastic approach based on Mesh Adaptive Direct Search Algorithm (MADS) that guarantees local optimality. It can be used to solve non-convex MINLP and has a relatively good performance.
GA [21]	A meta-heuristic stochastic approach that can be tuned to solve global optimization problems. We use Matlab *Optimization Toolbox*'s implementation.

A. Methodology

Performance metrics: Our primary metrics for comparisons are:

(1) The best solution to the objective function: Since obtaining the global optimum for the NP-hard problem is daunting, we are primarily interested in ϵ-global optimum;

(2) Convergence Time, which is the time an algorithm needs to obtain the best solution;

(3) Stability and Robustness, which is characterized by the frequency or ability of the algorithm to provide feasible solutions, provided that they are known to exist;

(4) Energy efficiency in joint optimization. We compare the energy cost of our joint optimization framework for communication, computation and caching (C3) with that of the optimization of any of the two types of resources (denoted by C2) under the same situation. The energy efficiency $\mathcal{E}$ defined as:

$$\mathcal{E} = \frac{E^{\text{total}*}(\text{C2}) - E^{\text{total}*}(\text{C3})}{E^{\text{total}*}(\text{C2})} \times 100\%, \tag{13}$$

where $E^{\text{total}*}(\text{C3})$ and $E^{\text{total}*}(\text{C2})$ are the optimal energy costs under the C3 optimization framework in (7) and the C2 optimization, respectively. $\mathcal{E}$ reflects the reduction of energy efficiency for the C3 over the C2 optimization.

Setup: We implement V-SBB in Matlab on a Core i7 3.40 GHz CPU with 16 GB RAM. The candidate MINLP solvers in this work include Bonmin, NOMAD and GA, which are implemented with Opti-Toolbox [31]. We summarize the characteristics of these solvers in Table II. Note that these solvers

TABLE III: Parameters used in simulations

Parameter	Value	Parameter	Value (Joules)
y_k	1000	ε_{vR}	50×10^{-9}
R_k	100	ε_{vT}	200×10^{-9}
w_{ca}	1.88×10^{-6}	ε_{cR}	80×10^{-9}
T	10s	γ	$[1, \sum_{k \in \mathcal{K}} y_k]$

TABLE IV: The Best Solution to the Objective Function (Obj.) and Convergence time for two nodes network

Solver	$\gamma = 1$		$\gamma = 250$		$\gamma = 500$		$\gamma = 750$		$\gamma = 1000$	
	Obj.	**Time** (s)	**Obj.**	**Time** (s)	**Obj.**	**Time** (s)	**Obj.**	**Time** (s)	**Obj.**	**Time** (s)
Bonmin	0.010	0.076	0.018	0.07	0.026	0.071	0.032	0.077	0.039	0.102
NOMAD	0.012	1.036	0.038	0.739	0.033	0.640	0.038	0.203	0.039	0.263
GA	0.010	0.286	0.018	2.817	0.026	7.670	0.042	11.020	0.064	3.330
V-SBB	0.010	18.231	0.018	17.389	0.026	12.278	0.032	7.327	0.039	19.437
Relaxed	0.010	0.075	0.018	0.048	0.026	0.046	0.032	0.050	0.039	0.059

can be applied directly to solve the original optimization problem in (7), while our V-SBB solves the equivalent problem. The reformulations needed are executed by a Java based module and we derive the bounds on the auxiliary variables. We also relax the integer constraint in (7) to obtain a non-linear programming problem, which is solved by IPOPT [32] and use it as a benchmark for comparison. V-SBB terminates when ϵ-optimality is obtained or a computation timer of 200 seconds expires. We take $\epsilon = 0.001$ in our study. If the timer expires, the last feasible solution is taken as the best solution. Our simulation parameters are provided in Table III, which are the typical values used in the literature [15], [33], [34].

B. The Best Solution to the Objective Function

We compare the performance of V-SBB with three other candidate solvers for the networks in Figure 3. The results for two nodes and seven nodes networks are presented in Tables IV and V. We also relax the integer constraint in (7) to be continuous, i.e., $b_{k,i} \in [0, 1]$. Then (7) becomes a geometric programming problem, which can be solved by IPOPT [32]. We call it "Relaxed" and the corresponding results are presented in the last row of Tables IV and V. We observe that V-SBB achieves the lowest value comparable to Bonmin for larger values of γ, and significantly outperforms Bonmin for smaller values of γ, which we discuss in detail later. However, Bonmin cannot generate a feasible solution even if it exists for some cases. This is because Bonmin is built on the Branch-and-Cut method, which sometimes

TABLE V: The Best Solution to the Objective Function (Obj.) and Convergence time for seven nodes network

Solver	$\gamma = 1$		$\gamma = 1000$		$\gamma = 2000$		$\gamma = 3000$		$\gamma = 4000$	
	Obj.	**Time** (s)	**Obj.**	**Time** (s)	**Obj.**	**Time** (s)	**Obj.**	**Time** (s)	**Obj.**	**Time** (s)
Bonmin	0.0002	0.214	0.039	0.164	0.078	0.593	0.117	0.167	0.156	0.212
NOMAD	0.004	433.988	0.121	381.293	0.108	203.696	0.158	61.093	0.181	26.031
GA	0.043	44.538	0.096	30.605	0.164	44.970	0.226	17.307	0.303	28.820
V-SBB	0.0001	1871.403	0.039	25.101	0.078	30.425	0.117	23.706	0.156	19.125
Relaxed	0.0002	0.201	0.039	0.111	0.078	0.095	0.117	0.102	0.156	0.105

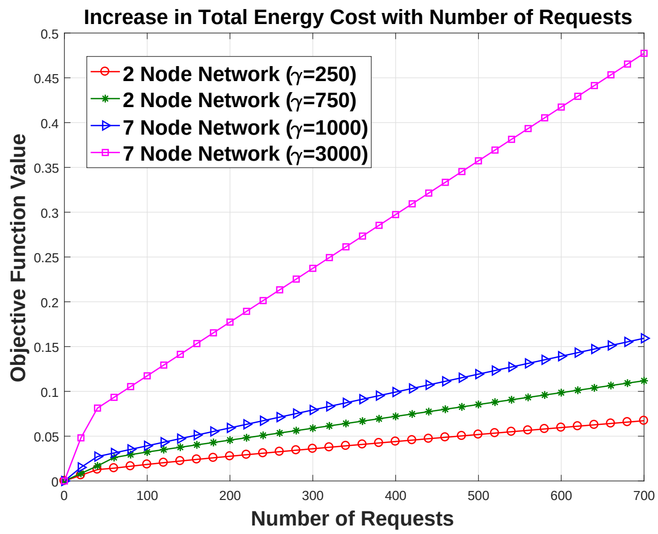

Fig. 4: Total Energy Costs vs. Number of Requests.

cuts regions where a lower value exists. NOMAD and GA in general yield a higher objective-function value than V-SBB does. This is because both NOMAD and GA are based on a stochastic approach which cannot guarantee convergence to the ϵ-global optimum. Similar trends are observed for three and four node networks, which are presented in Appendix E.

Figure 4 verifies that the optimal energy cost is monotonically increasing with the number of requests, as stated in Remark 1 for a two node and seven node network. The results are obtained using our C3 framework for $\gamma = 0.25 \sum_{k \in \mathcal{K}} y_k$ and $\gamma = 0.75 \sum_{k \in \mathcal{K}} y_k$, respectively. For the network parameters under consideration, we note that there is a turning point on the curves, and the total energy cost increases much faster with the number of requests before the turning point than that after it. This is because the data has already been cached at the root node at this point and there is no need to retrieve data from other nodes in the network, which reduces transmission costs. This is the benefit that caching brings, and we will further discuss the advantage of C3 optimization over the C2 later in Section V-E.

TABLE VI: Infeasibility of Bonmin for networks in Figure 3

Networks	(a)	(b)	(c)	(d)
# of test values	1000	2000	2000	4000
# of infeasible solutions	0	0	1	216
Infeasibility (%)	0	0	0.05	5.4

C. Convergence Time

The time taken to obtain the best solution is important in practice. The amount of time that an algorithm requires to obtain its best solution as discussed in Section V-B are shown in Tables IV and V for the two nodes and seven nodes networks, respectively. It can be see that Bonmin is the fastest method since it uses the branch-and-cut approach which cuts certain domains to accelerate the branching process. As discussed earlier, the Bonmin algorithm is fast at the expense of algorithm stability, i.e., sometimes it cannot find a solution although it exists. This will be further discussed in the following section. V-SBB takes longer to obtain a better solution, because our reformulation introduces auxiliary variables and additional linear constraints. Different applications can tolerate various degrees of algorithm speed. For the sample networks and applications under consideration, the speed of V-SBB is considered to be acceptable [24].

D. Stability

From the analysis in Sections V-B and V-C, we know that Bonmin is faster but unstable in some situations. We further characterize the stability of Bonmin with respect to the threshold value of QoI γ as follows. Specifically, we fix all other parameters in Table III, and vary only the maximal possible value of γ in different networks. The results are shown in Table VI. For each maximal value, we test all the possible integer values of γ between 1 and itself. Hence, the number of tests equals the maximal value. We see that the number of instances where the Bonmin method fails to produce a feasible solution increases as the network size increases. This is mainly due to the cutting phase in the Bonmin method, which cuts the feasible regions that need to be branched.

TABLE VII: Comparison between V-SBB and Bonmin for smaller values of γ in seven node network

Solver	γ =1		γ=3		γ =5		γ =8		γ =50	
	Obj.	**Time (s)**	**Obj.**	**Time**	**Obj.**	**Time**	**Obj.**	**Time**	**Obj.**	**Time**
Bonmin	0.0002	0.214	0.0003	0.211	0.0003	0.224	0.0005	0.23	0.0021	0.364
V-SBB	0.00011	1871.403	0.00015	2330	0.00019	1243.77	0.00047	1350.016	0.0020	3325.302
Improvement (%)	52.45		49.43		50.30		7.59		4.62	

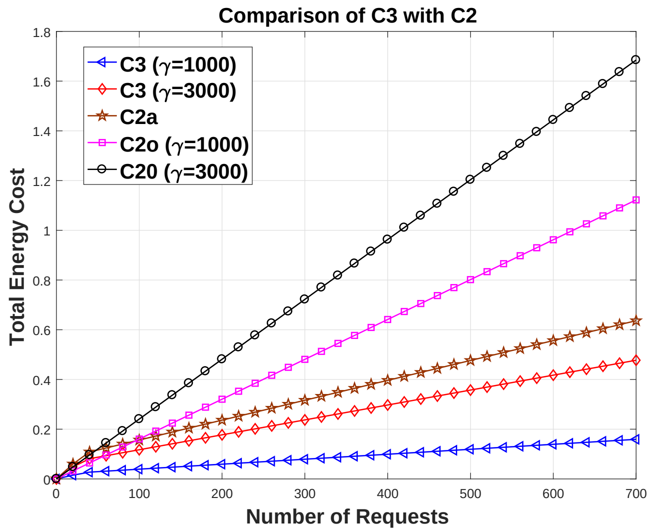

Fig. 5: Comparison of C3 and C2 optimization for the seven node network in Figure 3.

Although Bonmin can provide a feasible solution for smaller values of γ at a faster time, we observe that the value of the solution is larger than that of V-SBB. We compare the performance of V-SBB and Bonmin for smaller values of γ in Table VII. We see that V-SBB outperforms Bonmin by as much as 52.45% when searching for an ϵ-global optimum, though it requires more time. The timer is set to 7200s for results shown in Table VII.

E. Energy Efficiency

We compare the total energy costs under joint C3 optimization with those under C2 optimization. We consider two cases for the C2 optimization: (i) C2o (Communication and Computation), where we set $S_v = 0$ for each node to avoid any data caching; (ii) C2a (Communication and Caching), where we set $\gamma = \sum_{k \in \mathcal{K}} y_k$, which is equivalent to $\delta_v = 1$, $\forall v \in V$, i.e., no computation. Comparison between C3, C2o and C2a is shown in Figure 5.

First, we observe that as the number of requests increases, the total energy cost increases, as reflected in Remark 1. Second, the energy cost for the C3 joint optimization is lower than that for C2o optimization for the same parameter setting. This captures the tradeoff between caching, communication and computation. In other words, although C3 incurs caching costs, it may significantly reduce the communication and computation, which in turn brings down total energy cost. Similarly, C3 optimization outperforms C2a although C3 incurs caching cost. Using Equation (13), energy efficiency improves by as much as 88% for the C3 framework when compared with the C2 formulation. These trends are observed in other candidate network topologies. Details for the 2 node network can be found in Appendix F.

Remark 4. *Note that the above results are based on parameter values typically used in the literature, as shown in Table III. From our analysis, it is clear that the larger the ratio between ε_{vT} and ε_{vR}, ε_{vC}, the larger will be the improvement provided by our $C3$ formulation.*

VI. Related Work

A key focus of this work is to demonstrate and validate the joint application of data computation and caching, specifically in geo-distributed systems, e.g., WSNs, to achieve minimal energy consumption due to data communication, computation and caching with a QoI guarantee. Key decisions for a geo-distributed system are how much of the computation should be performed at each server and where the data should be cached in the system. The basic building blocks of our model are simple and have been studied in various settings. However, to the best of our knowledge, there is no prior work that jointly considers communication, computation and caching costs in data communication networks with a QoI guarantee for end users.

Data Compression: Compression is a key operator in data analytics and has been supported by many data-parallel programming models [3]. For WSNs, data compression is usually performed over a hierarchical topology to improve communication energy efficiency [12], whereas we focus on energy tradeoff between communication, computation and caching.

Data Caching: Caches play a significant role in many systems with hierarchical topologies, e.g., WSNs, microprocessors, CDNs etc. There is a rich literature on the performance of caching in terms of designing different caching algorithms, e.g., [23], [35]–[37], and we do not attempt to provide an overview here. Utility maximization approach has also been studied for cache management [38]–[40]. However, none of these work considered the costs of caching, which may be significant in some systems [16].

Energy Costs: While optimizing energy costs in wireless sensor networks has been extensively studied [33], [34], existing work primarily is concerned with routing [41], MAC protocols [33], and clustering [42]. With the growing deployment of smart sensors in modern systems [15], in-network data processing, such as data aggregation, has been widely used as a mean of reducing system energy cost by lowering the data volume for transmission.

Energy efficient inference in a random fusion network without QoI guarantee was considered in [43]. Network Utility Maximization (NUM) framework was applied in [22] to obtain optimal compression rate for data aggregation as well as optimal locations for performing data compression. The optimal energy allocation between communication and sensing to maximize the total information received at the sink node was studied in [44], but they did not consider data computation. An efficient algorithm for data compression in a data gathering tree was proposed in [45]. A distributed algorithm to minimize overall energy costs in a tree structured network by optimizing the compression factor at each node was presented in [15]. While these work only focus on energy costs of data communication and compression, we study the energy tradeoff between data communication, computation and caching.

VII. Conclusion

We have investigated energy efficiency tradeoffs among communication, computation and caching with QoI guarantee in distributed networks. We first formulated an optimization problem that characterizes these energy costs. This optimization problem belongs to the non-convex class of MINLP, which is hard to solve in general. We then proposed a variant of the spatial branch-and-bound (V-SBB) algorithm, which can solve the MINLP with ϵ-optimality guarantee. Finally, we showed numerically that the newly proposed V-SBB algorithm outperforms the existing MINLP solvers, Bonmin, NOMAD and GA. We also observed that C3 optimization framework, which to the best of our knowledge has not been investigated in the literature, leads to an energy saving of as much as 88% when compared with either of the C2 optimizations which have been widely studied.

Going further, we aim to extend our results in two ways. The first is to refine and improve the symbolic reformulation to reduce the number of needed auxiliary variables in order to shorten the algorithm execution time. Second, since many networking problems involve the optimization of both continuous and discrete variables as in this work, we plan to apply and extend the newly proposed V-SBB to solve those problems.

Acknowledgements

This work was supported by the U.S. Army Research Laboratory and the U.K. Ministry of Defence under Agreement Number W911NF-16-3-0001. The views and conclusions contained in this document are those of the authors and should not be interpreted as representing the official policies, either expressed or implied, of the U.S. Army Research Laboratory, the U.S. Government, the U.K. Ministry of Defence or the U.K. Government. The U.S. and U.K. Governments are authorized to reproduce and distribute reprints for Government purposes notwithstanding any copy-right notation hereon. Faheem Zafari also acknowledges the financial support by EPSRC Centre for Doctoral Training in High Performance Embedded and Distributed Systems (HiPEDS, Grant Reference EP/L016796/1), and Department of Electrical and Electronics Engineering, Imperial College London.

References

[1] B. Heintz, A. Chandra, and R. K. Sitaraman, "Trading Timeliness and Accuracy in Geo-Distributed Streaming Analytics," in *Proc. of SoCC*, 2016.

[2] B. Heintz, A. Chandra, and R. K. Sitaraman, “Optimizing Grouped Aggregation in Geo-Distributed Streaming Analytics,” in *Proc. of HPDC*, 2015.

[3] O. Boykin, S. Ritchie, I. O’Connell, and J. Lin, “Summingbird: A Framework for Integrating Batch and Online Mapreduce Computations,” *Proc. of VLDB*, 2014.

[4] T. E. Klein and P. Richard, “ICT energy challenges, impact and solutions,” in *19th International ICIN Conference-Innovations in Clouds, Internet and Networks*, 2016.

[5] https://www.theregister.co.uk/2013/08/16/it_electricity_use_worse_than_you_thought/.

[6] Nokia Bell Labs, https://www.bell-labs.com/var/articles/gwtt/.

[7] N. Dimokas, D. Katsaros, and Y. Manolopoulos, “Cooperative Caching in Wireless Multimedia Sensor Networks,” *Mobile Networks and Applications*, vol. 13, no. 3-4, pp. 337–356, 2008.

[8] N. Dimokas, D. Katsaros, L. Tassiulas, and Y. Manolopoulos, “High Performance, Low Complexity Cooperative Caching for Wireless Sensor Networks,” *Wireless Networks*, vol. 17, no. 3, pp. 717–737, 2011.

[9] M. Alipio, N. M. Tiglao, A. Grilo, F. Bokhari, U. Chaudhry, and S. Qureshi, “Cache-based Transport Protocols in Wireless Sensor Networks: A Survey and Future Directions,” *Journal of Network and Computer Applications*, 2017.

[10] J. Li, B. Liu, and H. Wu, “Energy-efficient in-network Caching for Content-Centric Networking,” *IEEE Communications Letters*, vol. 17, no. 4, pp. 797–800, 2013.

[11] G. F. Elmasry, “A Comparative Review of Commercial vs. Tactical Wireless Networks,” *IEEE Communications Magazine*, vol. 48, no. 10, 2010.

[12] R. Rajagopalan and P. K. Varshney, “Data Aggregation Techniques in Sensor Networks: A Survey,” *IEEE Commun. Surveys Tuts.*, vol. 8, no. 4, pp. 48–63, 2006.

[13] E. Fasolo, M. Rossi, J. Widmer, and M. Zorzi, “In-network Aggregation Techniques for Wireless Sensor Networks: a Survey,” *IEEE Wireless Communications*, vol. 14, no. 2, 2007.

[14] K. C. Barr and K. Asanović, “Energy-aware Lossless Data Compression,” *ACM Transactions on Computer Systems*, 2006.

[15] S. Nazemi, K. K. Leung, and A. Swami, “QoI-aware Tradeoff Between Communication and Computation in Wireless Ad-hoc Networks,” in *Proc. IEEE PIMRC*, 2016.

[16] N. Choi, K. Guan, D. C. Kilper, and G. Atkinson, “In-network Caching Effect on Optimal Energy Consumption in Content-Centric Networking,” in *Proc. IEEE ICC*, 2012.

[17] S. A. Ehikioya, “A Characterization of Information Quality Using Fuzzy Logic,” in *NAFIPS*, 1999.

[18] E. M. Smith and C. C. Pantelides, “Global Optimisation of General Process Models,” in *Glo. Opt. Eng. Des.* Springer, 1996, pp. 355–386.

[19] P. Bonami *et al.*, “An Algorithmic Framework for Convex Mixed Integer Nonlinear Programs,” *Disc. Opt.*, vol. 5, no. 2, pp. 186–204, 2008.

[20] S. Le Digabel, “Algorithm 909: NOMAD: Nonlinear Optimization with the MADS Algorithm,” *ACM TOMS*, vol. 37, no. 4, p. 44, 2011.

[21] K. Deb, A. Pratap, S. Agarwal, and T. Meyarivan, “A Fast and Elitist Multiobjective Genetic Algorithm: NSGA-II,” *IEEE transactions on evolutionary computation*, vol. 6, no. 2, pp. 182–197, 2002.

[22] S. Eswaran, J. Edwards, A. Misra, and T. F. L. Porta, “Adaptive In-Network Processing for Bandwidth and Energy Constrained Mission-Oriented Multihop Wireless Networks,” *IEEE Transactions on Mobile Computing*, vol. 11, no. 9, pp. 1484–1498, Sept 2012.

[23] S. Ioannidis and E. Yeh, “Adaptive Caching Networks with Optimality Guarantees,” in *ACM SIGMETRICS*, 2016.

[24] C. A. Floudas, *Deterministic Global Optimization: Theory, Methods and Applications*. Springer Science & Business Media, 2013, vol. 37.

[25] E. M. Smith and C. C. Pantelides, "A Symbolic Reformulation/Spatial Branch-and-Bound Algorithm for the Global Optimisation of Nonconvex MINLPs," *Comp. & Chem. Eng.*, vol. 23, no. 4, pp. 457–478, 1999.

[26] E. M. Smith, "On the Optimal Design of Continuous Processes," Ph.D. dissertation, Imperial College London (University of London), 1996.

[27] L. Liberti, "Reformulation and Convex Relaxation Techniques for Global Optimization," *4OR: A Quarterly Journal of Operations Research*, vol. 2, no. 3, pp. 255–258, 2004.

[28] L. Liberti, "Reformulation and Convex Relaxation Techniques for Global Optimization," Ph.D. dissertation, Imperial College London, 2004.

[29] G. P. McCormick, "Computability of Global Solutions to Factorable Nonconvex Programs: Part IConvex Underestimating Problems," *Mathematical Programming*, vol. 10, no. 1, pp. 147–175, 1976.

[30] T. Achterberg, "SCIP: Solving Constraint Integer Programs," *Mathematical Programming Computation*, vol. 1, no. 1, pp. 1–41, 2009.

[31] OPTI Toolbox, "A Free Matlab Toolbox for Optimization," https://www.inverseproblem.co.nz/OPTI/index.php/Main/HomePage, [Online; accessed 28-Jun-2017].

[32] A. Wächter and L. T. Biegler, "On the Implementation of an Interior-point Filter Line-search Algorithm for Large-scale Nonlinear Programming," *Mathematical Programming*, vol. 106, no. 1, pp. 25–57, 2006.

[33] W. R. Heinzelman, A. Chandrakasan, and H. Balakrishnan, "Energy-Efficient Communication Protocol for Wireless Microsensor Networks," in *System sciences*, 2000.

[34] W. Ye, J. Heidemann, and D. Estrin, "An Energy-Efficient MAC Protocol for Wireless Sensor Networks," in *IEEE INFOCOM*, 2002.

[35] M. Garetto, E. Leonardi, and V. Martina, "A Unified Approach to the Performance Analysis of Caching Systems," *ACM TOMPECS*, vol. 1, no. 3, p. 12, 2016.

[36] N. C. Fofack, P. Nain, G. Neglia, and D. Towsley, "Analysis of TTL-based Cache Networks," in *VALUETOOLS*, 2012.

[37] J. Li, S. Shakkottai, J. C. S. Lui, and V. Subramanian, "Accurate Learning or Fast Mixing? Dynamic Adaptability of Caching Algorithms," *Arxiv preprint arXiv:1701.02214*, 2017.

[38] M. Dehghan, L. Massoulie, D. Towsley, D. Menasche, and Y. Tay, "A Utility Optimization Approach to Network Cache Design," in *Proc. of IEEE INFOCOM*, 2016.

[39] N. K. Panigrahy, J. Li, and D. Towsley, "Hit Rate vs. Hit Probability Based Cache Utility Maximization," in *Proc. of ACM MAMA*, 2017.

[40] N. K. Panigrahy, J. Li, F. Zafari, D. Towsley, and P. Yu, "What, When and Where to Cache: A Unified Optimization Approach," *Arxiv preprint arXiv:1711.03941*, 2017.

[41] A. Manjeshwar and D. P. Agrawal, "TEEN: a Routing Protocol for Enhanced Efficiency in Wireless Sensor Networks," in *IPDPS*, 2001.

[42] M. Ye, C. Li, G. Chen, and J. Wu, "EECS: an Energy Efficient Clustering Scheme in Wireless Sensor Networks," in *IEEE IPCCC*, 2005.

[43] A. Anandkumar, J. E. Yukich, L. Tong, and A. Swami, "Energy Scaling Laws for Distributed Inference in Random Fusion Networks," *IEEE Journal on Selected Areas in Communications*, vol. 27, no. 7, 2009.

[44] C. Zhang, J. Kurose, Y. Liu, D. Towsley, and M. Zink, "A Distributed Algorithm for Joint Sensing and Routing in Wireless Networks with Non-steerable Directional Antennas," in *IEEE ICNP*, 2006.

[45] Y. Yu, B. Krishnamachari, and V. K. Prasanna, "Data Gathering with Tunable Compression in Sensor Networks," *IEEE Transactions on Parallel and Distributed Systems*, vol. 19, no. 2, pp. 276–287, 2008.

Appendix A

The optimization problem in (7) can be mapped into a general form non-convex MINLP (14) by

$$\begin{aligned} \min_{\mathbf{x},\mathbf{y}} \quad & f(\mathbf{x},\mathbf{y}), \\ \text{s.t.} \quad & \mathbf{h}(\mathbf{x},\mathbf{y}) = 0, \\ & \mathbf{g}(\mathbf{x},\mathbf{y}) \leq 0, \\ & \mathbf{x} \in \mathbf{X} \subseteq \mathbb{R}^n, \\ & \mathbf{y} \in \{0,1\}^q. \end{aligned} \tag{14}$$

- Transforming the first constraint in (7) into $\leq$ inequality. This can be achieved by multiplying both sides of the first constraint with -1. Then to match $g(x,y) \leq 0$, we add γ to both sides of constraint 1.
- Subtract S_v from both sides of constraint 3 and subtract 1 form both sides of constraint 4 in in (7).

Following above changes, (7) turns into

$$\begin{aligned} \min_{\boldsymbol{\delta},\boldsymbol{b}} \quad & E^{\text{total}}(\boldsymbol{\delta},\boldsymbol{b}) \\ \text{s.t.} \quad & -\sum_{k\in\mathcal{K}} y_k \prod_{i=0}^{h(k)} \delta_{k,i} + \gamma \leq 0, \\ & b_{k,i} \in \{0,1\}, \forall k \in \mathcal{K}, i = 0, \cdots, h(k), \\ & \sum_{k\in C_v} b_{k,h(v)} y_k \prod_{j=h(k)}^{h(v)} \delta_{k,j} - S_v \leq 0, \forall\, v \in V, \\ & \sum_{i=0}^{h(k)} b_{k,i} - 1 \leq 0, \forall k \in \mathcal{K}, \end{aligned} \tag{15}$$

where (15) follow the form of (14).

$$\begin{aligned} \min_{w} \quad & w_f \\ \text{s.t.} \quad & \sum_{k\in\mathcal{K}} y_k \overline{w}_{k,j}^{C_1} \geq \gamma, \\ & \sum_{k\in C_v} y_k \overline{w}_{k,i}^{C_2} \leq S_v, \forall\, v \in V, \\ & \sum_{i=0}^{h(k)} b_{k,i} \leq 1, \forall k \in \mathcal{K}, \end{aligned}$$

$$
\begin{aligned}
& b_{k,i} \in \{0,1\}, \forall k \in \mathcal{K}, i = 0, \cdots, h(k), \\
& \mathbf{w}^l \leq \mathbf{w} \leq \mathbf{w}^U,\ \forall k \in \mathcal{K}, i = 0, \cdots, h(k), \\
& w^b_{k,i} = \delta_{k,i} \times \overline{w}_{k,a},\ \forall k \in \mathcal{K}, i = 0, \cdots, h(k), \\
& w^f_{k,i} = \frac{\overline{w}_{k,a}}{\delta_{k,i}},\ \forall k \in \mathcal{K}, i = 0, \cdots, h(k), \\
& y_k b_{k,i} - \overline{w}^{C_2''}_{k,i} = 0,\ \forall k \in \mathcal{K}, i = 0, \cdots, h(k), \\
& \overline{w}^{C_2}_{k,i} = \overline{w}^{C_2''}_{k,i} \times \overline{w}^{C_2'}_{k,\beta},\ \forall k \in \mathcal{K}, i = 0, \cdots, h(k), \\
& \sum_{j=0}^{i-1} b_{k,j} - \widetilde{w}_{k,i} = 0,\ \forall k \in \mathcal{K}, i = 0, \cdots, h(k), \\
& \overline{\overline{w}}_{k,i} = \overline{w}_{k,a} \times \widetilde{w}_{k,i},\ \forall k \in \mathcal{K}, i = 0, \cdots, h(k), \\
& \overline{w}^b_{k,i} = w^b_{k,i} \times \widetilde{w}_{k,i},\ \forall k \in \mathcal{K}, i = 0, \cdots, h(k), \\
& \overline{w}^f_{k,i} = w^f_{k,i} \times \widetilde{w}_{k,i},\ \forall k \in \mathcal{K}, i = 0, \cdots, h(k), \\
& \prod_{m=i+1}^{h(k)} \delta_{k,m} = \overline{w}_{k,\underbrace{h(k)-2-i}_{a}} = \begin{cases} \delta_{k,h(k)} \times \delta_{k,h(k)-1}, & \forall a = 0 \\ \overline{w}_{k,a-1} \times \delta_{k,m}, & m + a = h(k) - 1 \\ \delta_{k,h(k)}, & \forall i = h(k) - 1, \end{cases} \\
& \prod_{i=0}^{h(k)} \delta_{k,i} = \overline{w}^{C_1}_{k,\underbrace{h(k)-1}_{j}} = \begin{cases} \delta_{k,h(k)} \times \delta_{k,h(k)-1}, & \forall j = 0 \\ \overline{w}^{C_1}_{k,j-1} \times \delta_{k,j+1}, & \forall j = 1 \cdots h(k) - 1 \\ \delta_{k,h(k)}, & \forall i = h(k), \end{cases} \\
& \prod_{j=h(k)}^{h(v)} \delta_{k,j} = \overline{w}^{C_2'}_{k,\underbrace{\tau-2}_{\beta}} = \begin{cases} \delta_{k,h(k)} \times \delta_{k,h(k)-1}, & \forall \beta = 0 \\ \overline{w}^{C_1}_{k,j-1} \times \delta_{k,j+1}, & \forall \beta > 0 \\ \delta_{k,h(k)}, & \forall \beta < 0, \end{cases} \\
& w_f = \sum_{k \in \mathcal{K}} \sum_{i=0}^{h(k)} y_k \left(\left(\varepsilon_{kR} \overline{w}_{k,a} + \varepsilon_{kT} w^b_{k,i} + \varepsilon_{kC} w^f_{k,i} - \varepsilon_{kc} \overline{w}_{ka} \right) + A + B \right), \\
& A = \varepsilon_{kR} R_k \overline{w}_{k,a} + \varepsilon_{kT} w^b_{k,i} + \varepsilon_{kc} R_k w^f_{k,i} - \varepsilon_{kC} R_k \overline{w}_{k,a} - \varepsilon_{kR} \overline{w}_{k,a} - \varepsilon_{kT} w^b_{k,i} - \varepsilon_{kC} w^f_{k,i} + \varepsilon_{kC} \overline{w}_{k,a}, \\
& B = -\varepsilon_{kR} R_k \overline{\overline{w}}_{k,i} - \varepsilon_{kT} R_k \overline{w}^b_{k,i} - \varepsilon_{kc} R_k \overline{w}^f_{k,i} + \varepsilon_{kC} R_k \overline{\overline{w}}_{k,i} + \varepsilon_{kR} \overline{\overline{w}}_{k,i} + \varepsilon_{kT} \overline{w}^b_{k,i} + \varepsilon_{kC} \overline{w}^f_{k,i} - \varepsilon_{kC} \overline{\overline{w}}_{k,i}.
\end{aligned}
\tag{16}
$$

APPENDIX B

A. Symbolic Reformulation

The first step of the symbolic reformulation is to represent the algebraic expression (objective function and constraints) using a binary tree as shown in Figure 6. Symbolic reformulation transforms the algebraic

TABLE VIII: Symbolic Reformulation Rules defined in [18] where X stands for expression, C stands for Constant and V stands for variable

Left Subtree Class	**Right Subtree Class**	**Binary Operator**	**New Variable Definition**	**New Linear Constraint**	**Binary Tree Class**
C	C	$\pm$			C
		$\times$			C
		$\div$			C
V	C	$\pm$			X
		$\times$			X
		$\div$			X
X	C	$\pm$			X
		$\times$			X
		$\div$			X
C	V	$\pm$			X
		$\times$			X
		$\div$	Linear Fractional		V
V	V	$\pm$			X
		$\times$	Bilinear		V
		$\div$	Linear Fractional		V
X	V	$\pm$			X
		$\times$	Bilinear	Left	X
		$\div$	Linear Fractional	Left	X
C	X	$\pm$			X
		$\times$			X
		$\div$	Linear Fractional	Right	V
V	X	$\pm$			X
		$\times$	Bilinear	Right	V
		$\div$	Linear Fractional	Right	V
X	X	$\pm$			X
		$\times$	Bilinear	Left, Right	V
		$\div$	Linear Fractional	Left, Right	V

expression represented as binary tree into a set of linear constraints that might involve some newly introduced variables. As our optimization problem (7) contains bilinear and linear fractional terms, the newly introduced auxiliary variables are therefore either products or ratios of other variables i.e. $w_i \equiv w_j w_k$ and $w_i \equiv \frac{w_j}{w_k}$. The rules for efficiently[6] achieving such transformation are presented in [18] part

[6]Keeping the number of newly introduced variables to minimum

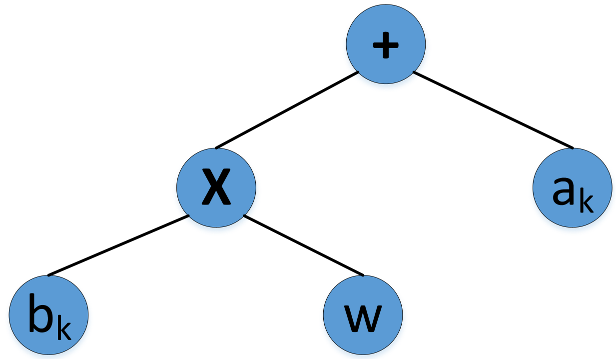

Fig. 6: Binary Tree representation for algebraic expression $b_k w + a_k$

of which we restate in the Table VIII. We create binary tree for representing the algebraic expressions and assign the leaf nodes a class that can be either a constant (C), an expression (X), or a variable (V). If we are at some intermediate node that represents a multiplication operation, and both its right and left child nodes are of class expression (X), then the reformulation would require us to introduce two linear constraints (for both right and left node explained) as well as introduce new bilinear auxiliary variable.

$$\begin{aligned}
\min_{\boldsymbol{w}} \quad & \boldsymbol{w}_f \\
\text{s.t.} \quad & \mathbf{A}\mathbf{w} = \mathbf{b}, \\
& \mathbf{w}^l \leq \mathbf{w} \leq \mathbf{w}^U, \\
& \mathbf{w}_k \equiv \mathbf{w}_i \mathbf{w}_j, \ \forall (i,j,k) \ \in \ \mathcal{T}_{\text{bt}}, \\
& \mathbf{w}_k \equiv \mathbf{w}_i / \mathbf{w}_j, \ \forall (i,j,k) \ \in \ \mathcal{T}_{\text{lft}}.
\end{aligned} \tag{17}$$

All the linear constraints are added into the constraint $Aw = b$ in (17) while the variables introduced are added into the vector $\mathbf{w}$ and depending on its type (either bilinear or linear fractional) its definition is added into either $\mathcal{T}_{\text{bt}}$ or $\mathcal{T}_{\text{lft}}$. After such reformulation, we obtain (17). The new variable vector $\mathbf{w}$ consists of continuous and discrete variables in the original MINLP, as well as other auxiliary variables introduced as a result of reformulation. The objective function w_f is a single auxiliary variable. This reformulation ensures that the new objective function and first constraint in (17) are linear, and all non-convexities and non-linearities in the original MINLP are absorbed by the sets $\mathcal{T}_{bt}$ and $\mathcal{T}_{lft}$.

B. Linear Constraint and Variable Creation

As seen in Table VIII, certain arithmetic operations during the symbolic reformulation require creation of new linear constraints and introduction of new variables. This can be easily explained by an example.

Let the parent node (any intermediate node that has 2 child nodes) represent a multiplication operation, the left subtree (child) be abc (expression where a,b are constants and c is a variable) and the right subtree be d (variable), then using the rules in the Table VIII, we need to introduce a new linear constraint (for the left subtree) and then a bilinear variable. So the linear constraint would be $abc - w(i) = 0$ where $w(i)$ is the i^{th} auxiliary variable introduced. The bilinear variable that has to be introduced would be $w(i+1) \equiv w(i)d$ where d is the variable in the original right subtree. The linear constraint will become part of of $Aw = b$ in (17) while $w(i+1)$ will be part of the set of binary terms $\mathcal{T}_{\text{bt}}$ If the intermediate node was a division operation, then we introduce the linear constraint just like we did for the multiplication operation, however we follow that by adding a linear fractional term $w(i+1) \equiv \frac{w(i)}{d}$. This is a recursive process and is repeated until all the terms in our objective function as well constraints are reformulated. Note that symbolic reformulation does not affect the linear terms in the original problem (7). Using this process, we reformulate (7) into (16) that can then be used with V-SBB.

Appendix C

A. Bilinear Terms

The McCormick linear overestimator and underestimator for bilinear terms with form $w_k \equiv w_i w_j$ are given by (18) and (19), respectively.

$$\begin{aligned} w_k &\leq w_i^l w_j + w_j^u w_i - w_i^l w_j^u, \\ w_k &\leq w_i^u w_j + w_j^l w_i - w_i^u w_j^l. \end{aligned} \tag{18}$$

$$\begin{aligned} w_k &\geq w_i^l w_j + w_j^l w_i - w_i^l w_j^l, \\ w_k &\geq w_i^u w_j + w_j^u w_i - w_i^u w_j^u. \end{aligned} \tag{19}$$

B. Linear Fractional Terms

The linear overstimator and underestimator for a linear fractional term withform $w_k \equiv \frac{w_i}{w_j}$ are similar to the overstimator and underestimator of bilinear terms given in (18) and (19). We first transform the linear fractional term into bilinear term, i.e., $w_i \equiv w_k w_j$ and then we can use (20) and (21) for the the linear overstimator and underestimator, respectively.

$$\begin{aligned} w_i &\leq w_k^l w_j + w_j^u w_k - w_k^l w_j^u, \\ w_i &\leq w_k^u w_j + w_j^l w_k - w_k^u w_j^l. \end{aligned} \tag{20}$$

$$w_i \geq w_k^l w_j + w_j^l w_k - w_k^l w_j^l,$$
$$w_i \geq w_k^u w_j + w_j^u w_k - w_k^u w_j^u. \tag{21}$$

The advantage of such linear understimator and overestimator is that even if the original problem is a non-convex MINLP, the relaxed problem will be an MILP which is comparatively easy to solve.

APPENDIX D

For the completeness, we present the following proofs for the convergence of spatial branch-and-bound [28], which work for our V-SBB.

Definition 2. *Let $\Omega \subseteq \mathbb{R}^n$. A finite family of sets $\mathcal{S}$ is a net for Ω if it is pairwise disjoint and it covers Ω.*

Definition 3. *A net $\mathcal{S}'$ is a refinement of the net $\mathcal{S}$ if there are finitely many pairwise disjoint $s'_i \in \mathcal{S}'$ such that $s = \bigcup_i s'_i \in \mathcal{S}$ and $s \notin S$.*

Definition 4. *Let $\mathcal{M}_n$ be an infinite sequence of subsets of x such that $\mathcal{M}_i \in \mathcal{S}_i$. $\mathcal{M}_n$ is a* filter *for $\mathcal{S}_n$ if $\forall i \in \mathbb{N}$ $\mathcal{M}_i \subseteq \mathcal{M}_{i-1}$ where $M_\infty = \bigcap_{i \in N} M_i$ be the limit of the filter.*

Definition 5. *Let $x \subseteq \mathbb{R}^n$ and $f(x)$ be the objective function of an MINLP problem then a spatial branch-and-bound algorithm would be convergent if $\gamma^* = \inf\ f(x) = \lim_{k\to\infty} \gamma_k$.*

Definition 6. *A selection rule is* exact *if*

1) *The infinimum objective function value of any region that remains qualified during the whole solution process is greater than or equal to the globally optimal objective function value, i.e.,*
$$\forall M \in \bigcap_{k=1}^{\infty} \mathcal{R}_k (\inf\ f(x \cap M) \geq \gamma^*)$$
2) *The limit $\mathbb{M}_\infty$ of any filter M_k is such that*$\inf f(\Omega \cap M) \geq \gamma^*$ *where Ω is the feasible set.*

Theorem 4. *A Spatial branch-and-bound algorithm using an exact selection rule converges.*

Proof. Proof by contradiction:

Let there be $x \in \Omega$ with $f(x) < \gamma^*$. Let $x \in M$ with $M \in \mathbb{R}_n$ for some $n \in \mathbb{N}$. Because of the first condition of exactness of selection rule, the filter M cannot remain qualified forever. Furthermore, unqualified regions may not, by hypothesis, include points with better objective function values than the current incumbent γ_k. Hence M must necessarily be split at some iteration $n' > n$ so x belongs to every $\mathcal{M}_n$ in some filter $\{\mathcal{M}_n\}$, thus $x \in \Omega \cap \mathbb{M}_\infty$. By condition 2 of exactness of selection rule, $f(x) \geq f(\Omega \cap M_\infty) \geq \gamma^*$. The result follows . $\square$

TABLE IX: The Value of Objective Function (Obj.) and Convergence Speed for three node network

Solver	$\gamma = 1$		$\gamma = 5000$		$\gamma = 10000$		$\gamma = 15000$		$\gamma = 20000$	
	Obj.	**Time** (s)	**Obj.**	**Time** (s)	**Obj.**	**Time** (s)	**Obj.**	**Time** (s)	**Obj.**	**Time** (s)
Bonmin	0.005	0.321	0.010	0.104	0.019	0.091	0.029	0.093	0.038	0.101
NOMAD	0.045	11.254	0.025	9.407	0.033	8.739	0.030	40.517	0.038	4.038
GA	0.025	0.509	0.010	9.799	0.027	4.924	0.045	19.045	0.050	2.154
Our	0.005	200	0.010	200	0.020	200	0.029	200	0.038	1.223
Relaxed	0.005	0.060	0.010	0.056	0.019	0.058	0.029	0.050	0.038	0.048

TABLE X: The Value of Objective Function (Obj.) and Convergence Speed for four node network

Solver	$\gamma = 1$		$\gamma = 5000$		$\gamma = 10000$		$\gamma = 15000$		$\gamma = 20000$	
	Obj.	**Time** (s)	**Obj.**	**Time** (s)	**Obj.**	**Time** (s)	**Obj.**	**Time** (s)	**Obj.**	**Time** (s)
Bonmin	0.002	0.337	0.020	0.104	0.040	0.104	0.059	0.100	0.079	0.139
NOMAD	0.003	101.891	0.023	90.626	0.040	52.293	0.060	47.068	0.104	2.070
GA	0.002	0.692	0.020	25.615	0.042	7.84	0.107	23.770	0.104	6.636
Our	0.002	200	0.020	200	0.052	200	0.059	200	0.079	13.344
Relaxed	0.002	0.500	0.020	0.066	0.040	0.062	0.059	0.073	0.079	0.083

Appendix E

The results for three nodes and four nodes networks are presented in Tables IX and X.

Appendix F

Figure 7 shows the improvement that C3 brings in comparison with C2 for a two nodes network. Using Equation (13), energy efficiency improves by as much as 70% for the C3 framework when compared with the C2 formulation.

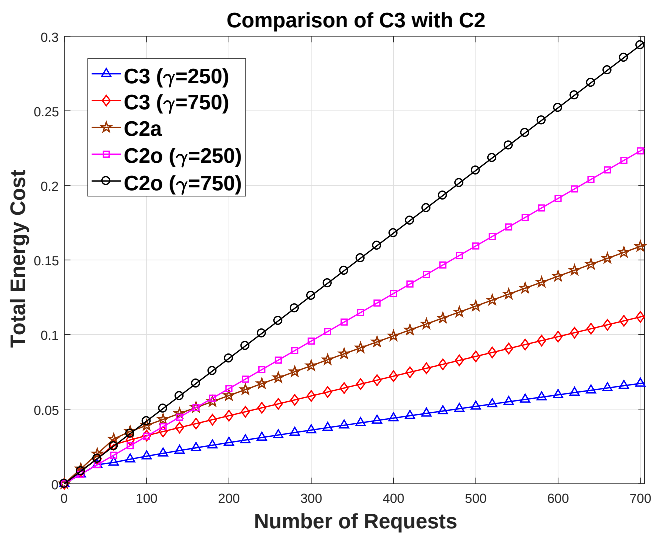

Fig. 7: Comparison of C3 and C2 optimization for the two nodes network in Figure 3.